

Cite this: *Chem. Sci.*, 2023, 14, 4901

All publication charges for this article have been paid for by the Royal Society of Chemistry

Received 2nd January 2023  
Accepted 3rd April 2023

DOI: 10.1039/d3sc00009e

rsc.li/chemical-science

# A photoluminescence assay with a portable device for rapid, sensitive and selective detection of europium and terbium†

Dipankar Bhowmik  and Uday Maitra \*

Rare earth elements are essential in many real-life applications, but their steady supply is being affected by multiple challenges. The recycling of lanthanides from electronic and other waste is thus gaining momentum which makes the detection of lanthanides with high sensitivity and selectivity a critical area of research. We now report a paper-based photoluminescent sensor for the rapid detection of terbium and europium with low detection limit (nM), which has the potential to facilitate recycling processes.

Rare earth elements (lanthanides, REEs) have unique optical, electrical, and magnetic characteristics and are essential for numerous advanced applications in electronics, catalysis, magnets, medical diagnosis, agriculture, and other fields.<sup>1,2</sup> Lanthanides are considered critical resources by the European Commission and the U. S. Department of Energy (DOE).<sup>3,4</sup> A stable and smooth supply of lanthanides is therefore essential for industries.

Lanthanide extraction and the subsequent separation from the co-mined element ores are associated with various challenges, which have necessitated the diversification of lanthanide sources and raised the concern of the recycling strategy. To accomplish efficient recovery of lanthanides from industrial<sup>5</sup> and domestic wastes<sup>6</sup> and mine drainage,<sup>7</sup> appropriate sensors with high sensitivity are required. The development of a lanthanide sensor providing low-cost, sensitive, and rapid analysis is thus critical in determining whether sufficient lanthanide is present in a sample to warrant extraction. Photoluminescent sensing methods have advantages for lanthanide detection due to their high sensitivity, portability, rapid measurement time, and low instrument cost.<sup>8–10</sup> Lanthanides have inherently sharp, almost line-like emission bands involving 4f–4f transitions, as the 4f orbital is effectively shielded by 5s and 5p orbitals. Consequently, element-specific emission bands make lanthanides excellent analytes for photoluminescence-based detection.

Using a paper-based sensing strategy, we have developed a photoluminescent lanthanide sensor to detect terbium and europium ions in a gel matrix. Table 1 highlights the significance of our protocol, with sensitivity over two orders of magnitude higher than other published methods for Eu<sup>3+</sup>.<sup>8,11–19</sup>

Department of Organic Chemistry, Indian Institute of Science, Bangalore 560012, Karnataka, India. E-mail: maitra@iisc.ac.in

† Electronic supplementary information (ESI) available. See DOI: <https://doi.org/10.1039/d3sc00009e>

The luminescence behaviour of lanthanides is controlled by three types of transitions: LMCT, 4f–5d transitions, and 4f–4f transitions.<sup>2,20</sup> The lower energy 4f–4f transitions have low absorption coefficients (typically <3 M<sup>-1</sup> s<sup>-1</sup>).<sup>21</sup> This problem has been addressed by positioning an organic chromophore close to the lanthanides where part of the energy absorbed by the organic moiety can be transferred to the lanthanide ion to generate its excited state(s), thus resulting in significantly enhanced sensitized emission through the ‘antenna effect’.<sup>22,23</sup>

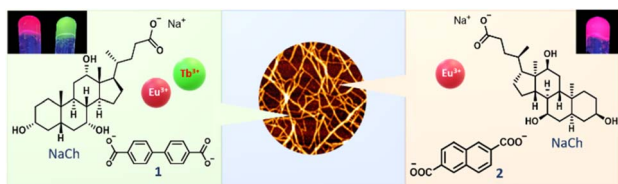
During the past decade, we have demonstrated a new strategy to enable emission from lanthanides in a hydrogel through a non-covalently-bound chromophore. This was achieved by doping appropriate chromophores in lanthanide cholate gels.<sup>24,25</sup> We have now discovered that dicarboxylic acid-based organic chromophores in the lanthanide cholate gels can also enable luminescence enhancement from multiple lanthanides (Scheme 1).

The sodium salt of biphenyl-4,4'-dicarboxylic acid (1) and naphthalene-2,6-dicarboxylic acid (2) was found to be effective sensitizers for lanthanides in their respective lanthanide

Table 1 Reported Limits of Detection (LOD) values of some colorimetric and fluorimetric probes for sensing Eu<sup>3+</sup>

Method	LOD (μM)	Ref.
Colorimetric	0.05	14
Photoluminescence	0.5	13
Photoluminescence	1.25	15
Colorimetric	3	16
Colorimetric	2	18
Photoluminescence	0.28	12
Photoluminescence	5	11
Photoluminescence	5	17
Photoluminescence	10	8
Photoluminescence	0.11	19
<b>Photoluminescence</b>	<b>0.0003</b>	<b>This work</b>





**Scheme 1** Schematic representation of sensitization of  $\text{Tb}^{3+}$  and  $\text{Eu}^{3+}$  using dicarboxylic acid-based organic chromophores in the metal-cholate hydrogel.

cholate ( $\text{LnCh}$ ) hydrogels. Among these chromophores, **1** exhibited high sensitization efficiency towards  $\text{Tb}^{3+}$  and  $\text{Eu}^{3+}$  when doped in micromolar concentrations. For example, terbium cholate ( $\text{TbCh}$ ) and europium Cholate ( $\text{EuCh}$ ) gels doped with  $200 \mu\text{M}$  of **1** showed 264-fold and 39-fold emission enhancement (compared to the native  $\text{TbCh}$  and  $\text{EuCh}$  gels), respectively, when excited at  $295 \text{ nm}$  (Fig. 1 and S1 ESI†). On the other hand, compound **2** at  $200 \mu\text{M}$  showed 155-fold  $\text{Eu}^{3+}$  emission enhancement, compared to only 4-fold for  $\text{Tb}^{3+}$ , thus showing a high selectivity towards  $\text{Eu}^{3+}$ . Lifetime and quantum yield of sensitized  $\text{Tb}^{3+}$  and  $\text{Eu}^{3+}$  emissions were calculated, and the lifetimes were found to be in the millisecond to sub-millisecond ranges (Fig. S2, Tables S1 and S2 ESI†).

Sensitization of lanthanide luminescence depends on the energy transfer from the ligand triplet state to the trivalent lanthanide ions. The sensitization by **1** and **2** can be interpreted in terms of coordination to  $\text{Eu}^{3+}/\text{Tb}^{3+}$  ions, the absorption of light, and triplet energy transfer. A good match of the absorption spectra (Fig. 1a–c) with the excitation spectra provides evidence for energy transfer from the organic chromophore to lanthanides, resulting in strong luminescence from the metal centre. Therefore, the sensitization of  $\text{Tb}^{3+}$  and  $\text{Eu}^{3+}$  by **1** and **2** depends on a delicate balance between the energy levels of the

sensitizer and these lanthanides and only some selective sensitizer molecules can lead to the sensitization of the lanthanide (Fig. S7 and S8 ESI†).

The significant luminescence enhancement of the lanthanide ions in cholate hydrogels suggested an indirect way of sensing such a lanthanide through a displacement assay using cholate gel derived from a non-photoluminescent metal ion. Several metal cholate gels were tested as the host matrix for the detection of lanthanides. The highest sensitivity was observed in lanthanum and yttrium cholate ( $\text{YCh}$ ) gels (Fig. S3 ESI†). Yttrium cholate gel was chosen as a host matrix as yttrium is less expensive and more abundant than lanthanum. Another reason for choosing  $\text{YCh}$  gel as a host matrix is that the morphology and mechanical properties of  $\text{YCh}$  gel were very similar to those of the lanthanide cholate gels (Fig. 2a–e).<sup>26,27</sup> To simplify the detection, the sensing experiment was performed on paper discs coated with the gel. It is well known that high energy O–H vibrations of water molecules lead to the quenching of  $\text{Ln}^{3+}$  luminescence.<sup>28</sup> We have observed that higher luminescence from lanthanide cholates can be achieved on paper, possibly because of the absorption of excess water from the gel matrix.<sup>29</sup> Additionally, paper makes the sensing technique more rapid, robust, sensitive, affordable, and user-friendly.<sup>26,30</sup> The gels ( $400 \mu\text{L}$ ) were prepared by mixing equal volumes of aqueous yttrium nitrate ( $10 \text{ mM}$ ) and  $\text{NaCh}$  ( $30 \text{ mM}$  with  $400 \mu\text{M}$  sensitizers **1** or **2**), with  $20 \mu\text{L}$  of analytes of various concentrations. Circular paper discs were made from western blotting paper ( $0.83 \text{ mm}$  thick) using a hole punch (diameter =  $0.45 \text{ cm}$ ), which was placed in a 96-multi well plate. The gel ( $20 \mu\text{L}$ ) was drop cast uniformly on the paper discs and air-dried for  $5 \text{ min}$  when the excess water of the gel was found to have been absorbed by the filter paper (Fig. S9 ESI†). The luminescence of sensitizer-doped  $\text{YCh}$  gels luminescence was checked on a plate reader. With the excitation and lanthanide emission information in hand, limits of detections (LOD) were estimated with **1**

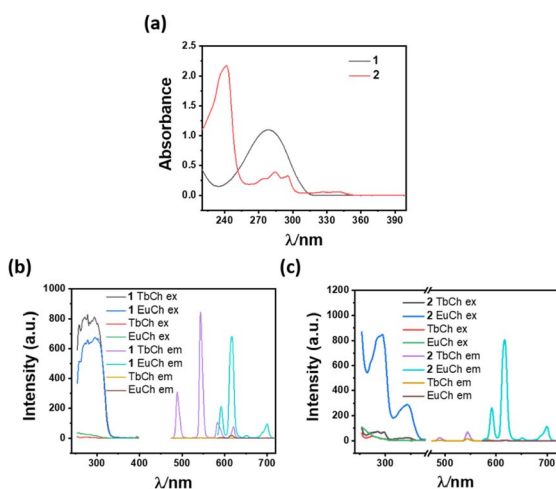


**Fig. 1** (a) Absorption spectra of  $100 \mu\text{M}$  sensitizers (**1**, **2**) in  $\text{H}_2\text{O}$ . (b) Sensitization of  $\text{Tb}^{3+}$  and  $\text{Eu}^{3+}$  in the presence of  $200 \mu\text{M}$  of **1** in the  $\text{TbCh}$  and  $\text{EuCh}$  gels, respectively ( $\lambda_{\text{ex}}$   $295 \text{ nm}$ ). (c) Sensitization of  $\text{Tb}^{3+}$  and  $\text{Eu}^{3+}$  in the presence of  $200 \mu\text{M}$  **2** in  $\text{TbCh}$  and  $\text{EuCh}$  gels, respectively ( $\lambda_{\text{ex}}$   $297 \text{ nm}$ ).

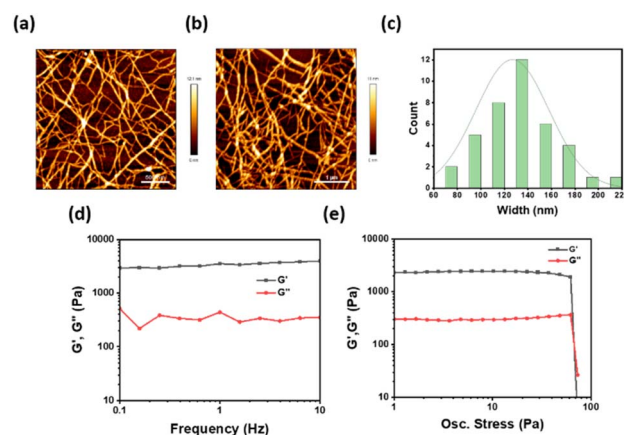


**Fig. 2** AFM images of (a) ( $5/15 \text{ mM}$ )  $\text{YCh}$  gel. (b)  $500 \mu\text{M}$   $\text{Eu}^{3+}$  doped ( $5/15 \text{ mM}$ )  $\text{YCh}$  gel. (c) Width distribution analyses of the  $\text{YCh}$  gel fibers from AFM images (number of bundled fibers counted for width distribution analyses 50). Rheology for ( $5/15 \text{ mM}$ )  $\text{YCh}$  hydrogels (d) frequency sweep at fixed stress of  $1.0 \text{ Pa}$ , (e) Stress sweep at a fixed frequency of  $1.0 \text{ Hz}$  at  $298 \text{ K}$ .



and 2 doped YCh gel-coated paper discs (Fig. 3, S4 and S5 ESI†). The same experimental technique was applied for the detection of both lanthanides. Each data point in the LOD plots is an average of at least four replicate measurements. A low nanomolar LOD was obtained for each lanthanide. Representative plots of concentration *versus* emission signal for LOD estimation are shown in Fig. 3.

At lower concentrations, a good linear relationship was achieved between the luminescence intensities at 545 nm and 617 nm and the concentrations of Tb<sup>3+</sup> and Eu<sup>3+</sup>, respectively (Fig. 3a–c, S4 and S5 ESI†). From these data, the limits of detection were calculated. The strong emission of REEs in the YCh gel suggests that YCh gel is an excellent host matrix used in the quantitative detection of trace amounts of REE. The standard deviation in the slope of each data point is nominal which implies the reliability of LOD estimated from the concentration *vs.* emission signal plots for each lanthanide.

We aimed here to test the response of each sensor to different lanthanides. 200 μM **1** was doped in the (5/15 mM) YCh gel for detection of Tb<sup>3+</sup> and Eu<sup>3+</sup> and the LOD value was found 7 and 5 nM respectively. Similarly, **2** was doped into the YCh gel for selective detection of Eu<sup>3+</sup>. Remarkably, sub-nanomolar (0.3 nM) LOD was achieved for Eu<sup>3+</sup> with **2** doped YCh gel.

These data, of course, represent the “best case” scenario in which no interferents are present. For an application involving mine drainage or other wastes, several potential interferents may complicate the sensor performance. To get early insight into the impact of the interferents on the performance of our probes in a “real life” sample, some control studies were performed with a high concentration of other metal ions. To check the potential of the sensor, several monovalent, divalent, and trivalent metal ions were added along with the Eu<sup>3+</sup>, and the role of other metal ions from the mixture system was checked. The potential interferents were separately mixed with Eu<sup>3+</sup> (10 :

1 ratio) and the luminescence response was checked in 200 μM **2** doped YCh gel. The interferent metal (20 μM) was mixed with an equal volume of 2 μM of Eu<sup>3+</sup> and 20 μL of the resulting solution was mixed with 400 μL of NaCh and Y(NO<sub>3</sub>)<sub>3</sub> solution and gels were prepared as before. These representative data (Fig. 4) suggest that no significant interference of the lanthanide detection in the presence of the excess additives.

Tb<sup>3+</sup> to Eu<sup>3+</sup> energy transfer has been reported in various systems such as in coordination polymers, lanthanide-based polymers, supramolecular gels, lanthanide nanoparticles, *etc.* Tb<sup>3+</sup> and Eu<sup>3+</sup> were mixed with a 1 : 1 ratio (up to 2 μM) in the 200 μM **2** doped YCh gel during gel formation. Europium luminescence was checked in the presence of terbium metal ions. No significant luminescence change was observed which implies the selective sensing of Eu<sup>3+</sup> metal ion from a Tb<sup>3+</sup>/Eu<sup>3+</sup> mixture at low concentrations. Therefore, we explored the selective quantitative detection of Eu<sup>3+</sup> metal ions from Tb<sup>3+</sup>/Eu<sup>3+</sup> mixtures (Table S3 and Fig S6 ESI†).

We have also designed and tested the first-generation prototype of a novel low-cost multiparametric, stand-alone imaging instrument for lanthanide detection. This compact device (18 × 18 cm<sup>2</sup>, <500 g weight) consists of excitation LEDs, a camera and image processing software to control the operation of the equipment from a touchscreen. A choice of three LEDs (275 nm, 310 nm, and 340 nm) focuses the excitation beam on the gel-coated paper discs. A digital image sensor captures the emitted light (620 nm) and the images are processed by the App.<sup>31</sup> Compound-**1** doped YCh gel was checked for the detection of Eu<sup>3+</sup> and the results confirmed the usefulness of the imaging device for several small and biomolecular detection, or fast *in loco* preliminary analyses without the aid of a specialized laboratory (Fig. 5).

In conclusion, we have reported two carboxylic acid-derived sensitizer molecules which sensitize emission from Tb<sup>3+</sup> and Eu<sup>3+</sup> metal ions. The lanthanide-sensitized luminescence was further used for detecting REEs in nanomolar and sub-nanomolar concentrations by a displacement assay using non-emissive Y-cholate gel as the platform. To make the detection

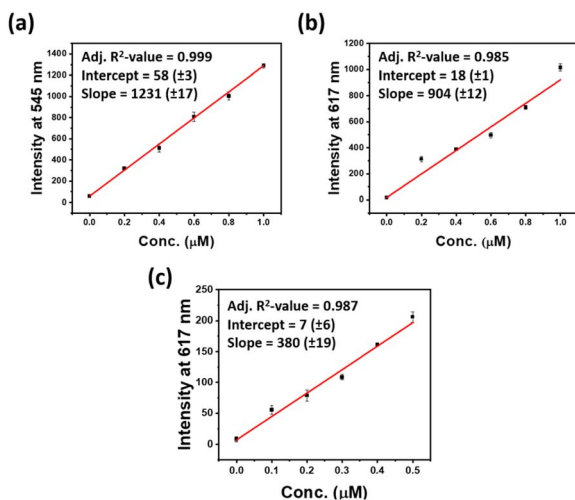


Fig. 3 Time-delayed (delay time: 0.2 ms, gate time: 3.0 ms) emission intensity ( $n = 4$ ) of gel-coated paper discs. (a) 20 μL 200 μM **1** doped YCh gel for Tb<sup>3+</sup> detection. (b) 20 μL 200 μM **1** doped YCh gel for Eu<sup>3+</sup> detection. (c) 20 μL 200 μM **2** doped YCh gel for Eu<sup>3+</sup> detection (with  $\lambda_{\text{ex}} = 295$  nm,  $\lambda_{\text{em}} = 545$  nm for Tb<sup>3+</sup> and  $\lambda_{\text{em}} = 617$  nm for Eu<sup>3+</sup>).

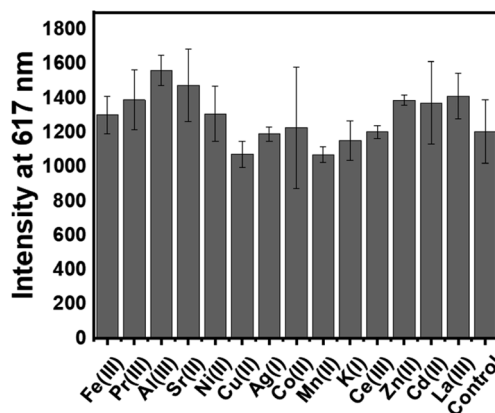


Fig. 4 Time-delayed emission intensity ( $n = 4$ ) of paper discs for the mixture of other metal ions ( $M^{n+}$ ) with Eu<sup>3+</sup> (10 : 1);  $M^{n+}$  conc. 10 μM, Eu<sup>3+</sup> (conc. 1 μM), with  $\lambda_{\text{em}} = 617$  nm and  $\lambda_{\text{ex}} = 297$  nm.



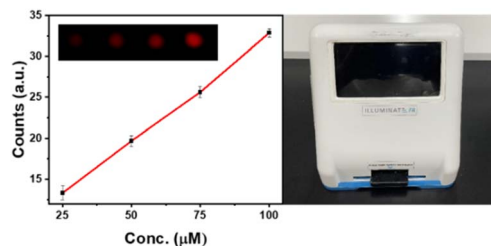


Fig. 5 Time-delayed emission intensity ( $n = 4$ ) of gel-coated paper discs, (left) 20  $\mu\text{L}$  200  $\mu\text{M}$  1 doped YCh gel for  $\text{Eu}^{3+}$  detection (with  $\lambda_{\text{ex}}$  270 nm,  $\lambda_{\text{em}}$  600 nm); (right) image of the portable device.

technique rapid and cost-effective, we developed a paper-based sensor. This system was found to be very selective and sensitive, and we could detect selectively  $\text{Eu}^{3+}$  from other metal mixtures. We believe that the protocol developed by us will provide a practical solution for lanthanide detections in a variety of industrial wastes and mine drainage. We are currently exploring the sensitization of other lanthanides in near-infrared (NIR) region with the sensitizer 1 and 2, which will be reported in due course.

## Data availability

All the relevant experimental data have been provided in the manuscript and in the ESI† document.

## Author contributions

DB and UM designed the experiments, and DB carried out all the experimental work. The analysis of the data and the manuscript writing were done by DB and UM.

## Conflicts of interest

There are no conflicts to declare.

## Acknowledgements

This work was financially supported by a research grant (#CRG/2021/1140) from the Science and Engineering Research Board (SERB), New Delhi. UM also thanks the SERB for the award of a J.C. Bose Fellowship (SR/S2/JCB-68/2007). The Council of Scientific and Industrial Research (CSIR) is thanked for the award of a research fellowship to DB. DB thanks Arnab Dutta for his assistance in carrying out some experiments described in Fig. 4. We also thank Adiuvio Diagnostics, Chennai for the fabrication of the imaging device with our specifications.

## Notes and references

- J. C. G. Bunzli, *Chem. Rev.*, 2010, **110**, 2729.
- S. V. Eliseeva and J. C. G. Bunzli, *Chem. Soc. Rev.*, 2010, **39**, 189.
- G. Blengini, C. El Latunussa, U. Eynard, C. Torres De Matos, D. Wittmer, K. Georgitzikis and C. Pavel, *Study on the EU's list*

of critical raw materials (2020), Final report, Publications Office, 2020.

- S. Chu, *Critical materials strategy*, DIANE publishing, 2011.
- P. Westerhoff, S. Lee, Y. Yang, G. W. Gordon, K. Hristovski, R. U. Halden and P. Herckes, *Environ. Sci. Technol.*, 2015, **49**, 9479.
- R. Lin, Y. Soong and E. J. Granite, *Int. J. Coal Geol.*, 2018, **192**, 1.
- C. Ayora, F. Macias, E. Torres, A. Lozano, S. Carrero, J. M. Nieto, R. Perez-Lopez, A. Fernandez-Martinez and H. Castillo-Michel, *Environ. Sci. Technol.*, 2016, **50**, 8255.
- A. E. Sedykh, J. J. Pflug, T. C. Schafer, R. Bissert, D. G. Kurth and K. Muller-Buschbaum, *ACS Sustainable Chem. Eng.*, 2022, **10**, 5101.
- R. M. Pallares, M. Charrier, S. Tejedor-Sanz, D. Li, P. D. Ashby, C. M. Ajo-Franklin, C. Y. Ralston and R. J. Abergel, *J. Am. Chem. Soc.*, 2022, **144**, 854.
- R. M. Pallares, D. D. An, P. Tewari, E. T. Wang and R. J. Abergel, *ACS Sens.*, 2020, **5**, 1281.
- S. Wang, L. Ding, J. Fan, Z. Wang and Y. Fang, *ACS Appl. Mater. Interfaces*, 2014, **6**, 16156.
- S. E. Crawford, X. Y. Gan, P. C. K. Lemaire, J. E. Millstone, J. P. Baltrus and P. R. Ohodnicki, *ACS Sens.*, 2019, **4**, 1986.
- P. J. J. Huang, J. Lin, J. Cao, M. Vazin and J. Liu, *Anal. Chem.*, 2014, **86**, 1816.
- C. E. Lisowski and J. E. Hutchison, *Anal. Chem.*, 2009, **81**, 10246.
- J. C. Ahern, Z. L. Poole, J. Baltrus and P. R. Ohodnicki, *IEEE Sens. J.*, 2017, **17**, 2644.
- R. M. Pallares, K. P. Carter, S. E. Zeltmann, T. Tratnjek, A. M. Minor and R. J. Abergel, *Inorg. Chem.*, 2020, **59**, 2030.
- J. A. Mattocks, J. V. Ho and J. A. Cotruvo, *J. Am. Chem. Soc.*, 2019, **141**, 2857.
- C. Hogendoorn, P. Roszczenko-Jasinska, N. C. Martinez-Gomez, J. de Graaff, P. Grassl, A. Pol, H. J. M. Op den Camp and L. J. Daumann, *Appl. Environ. Microbiol.*, 2018, **84**, e02887.
- X. X. Liu, L. P. Lu and M. L. Zhu, *Sens. Actuators, B*, 2021, **347**, 130641.
- P. Dorenbos, *J. Phys.: Condens. Matter*, 2003, **15**, 575.
- J. C. G. Bunzli and C. Piguet, *Chem. Soc. Rev.*, 2005, **34**, 1048.
- J. Georges, *Analyst*, 1993, **118**, 1481.
- E. S. Andreiadis, N. Gauthier, D. Imbert, R. Demadrille, J. Pecaut and M. Mazzanti, *Inorg. Chem.*, 2013, **52**, 14382.
- S. Banerjee, R. Kandanelli, S. Bhowmik and U. Maitra, *Soft Matter*, 2011, **7**, 8207.
- S. Bhowmik, S. Banerjee and U. Maitra, *Chem. Commun.*, 2010, **46**, 8642.
- D. Bhowmik, A. Dutta and U. Maitra, *Chem. Commun.*, 2020, **56**, 12061.
- A. Dutta and U. Maitra, *ACS Sens.*, 2022, **7**, 513.
- T. Forster, *Discuss. Faraday Soc.*, 1959, **27**, 7.
- R. Laishram and U. Maitra, *Chem. Commun.*, 2022, **58**, 3162.
- T. Gorai and U. Maitra, *ACS Sens.*, 2016, **1**, 934.
- The hardware and the software of this prototype are being optimized for the detection of both  $\text{Eu}^{3+}$  and  $\text{Tb}^{3+}$  photoluminescence. Once thorough testing is done, the technical details will be reported elsewhere.

